T H E U N I V E R S I T Y O F M I C H I G A N

COLLEGE OF ENGINEERING
Department of Electrical Engineering
Space Physics Research Laboratory

Final Report

HEMISPHERICAL LANGMUIR PROBE MEASUREMENTS IN THE LOWER IONOSPHERE

Y. S. Hsu
A. F. Nagy

ORA Project 07084

under contract with:

DEPARTMENT OF THE ARMY
BALLISTIC RESEARCH LABORATORIES
CONTRACT NO. DA-20-018-AMC-1765 (x)
ABERDEEN PROVING GROUND, MARYLAND

administered through:

OFFICE OF RESEARCH ADMINISTRATION ANN ARBOR

August 1967

TABLE OF CONTENTS

LIST OF TABLES

LIST OF FIGURES

I. INTRODUCTION

This is the final report on the Langmuir probe system which was developed and built by this Laboratory for the Ballistic Research Laboratory under Contract No. DA-20-018-AMC-1765(x), and was carried aboard Black Brant AC 17.604 launched from Fort Churchill at 12:16 P.M. on September 28, 1966, during a PCA event of about 1.5 db. The rocket reached an altitude of approximately 116 km. The primary mission of this experiment was to measure charged particle parameters in the D and lower E regions of the ionosphere during an auroral absorption event. The first part of this report deals with the engineering aspect of the probe system. In the next section the lack of an appropriate theory for supersonic D-region probes is discussed and the somewhat empirical approach used for the data reduction is outlined. In Section IV the data obtained from the probe results are shown and compared with the results of other experiments flown on the same rocket.

II. ENGINEERING ASPECTS

A. GENERAL DESCRIPTION

The Langmuir probe is but one of many experiments carried aboard the Black Brant Rocket AC 17.604 for making measurements in the D and lower E regions of the earth's ionosphere. The general payload layout and location of the various sensors is shown in Fig. 1. A more detailed description of the complete instrumentation of AC 17.604 was given by Burt.[1]

The velocity of the rocket is expected to be supersonic, resulting in the formation of a bow shock wave; therefore, it is important to locate the probe outside the influence of the shock cone of the rocket. The nose tip location was selected because of the technical advantages over a boom supported probe. Choice of a hemispherical over a conical configuration was influenced by the following considerations: (a) the effective collection area is not very sensitive to small changes in the angle of attack as would be the case for a conical nose tip and (b) the current collection theory for spherical collectors for long mean free path is well established.

Figures 2 and 3 show, respectively, the completely assembled Langmuir probe system and the system electronics with the housing removed. The Langmuir probe system used two VCO channels at 30 and 40 KHz and the system block diagram is shown in Fig. 4. The Langmuir probe current is measured alternately by the two channels, such that during the time when one channel is making current measurements the other channel performs inflight calibration and records other pertinent system parameters. The system logic timing and flags are shown

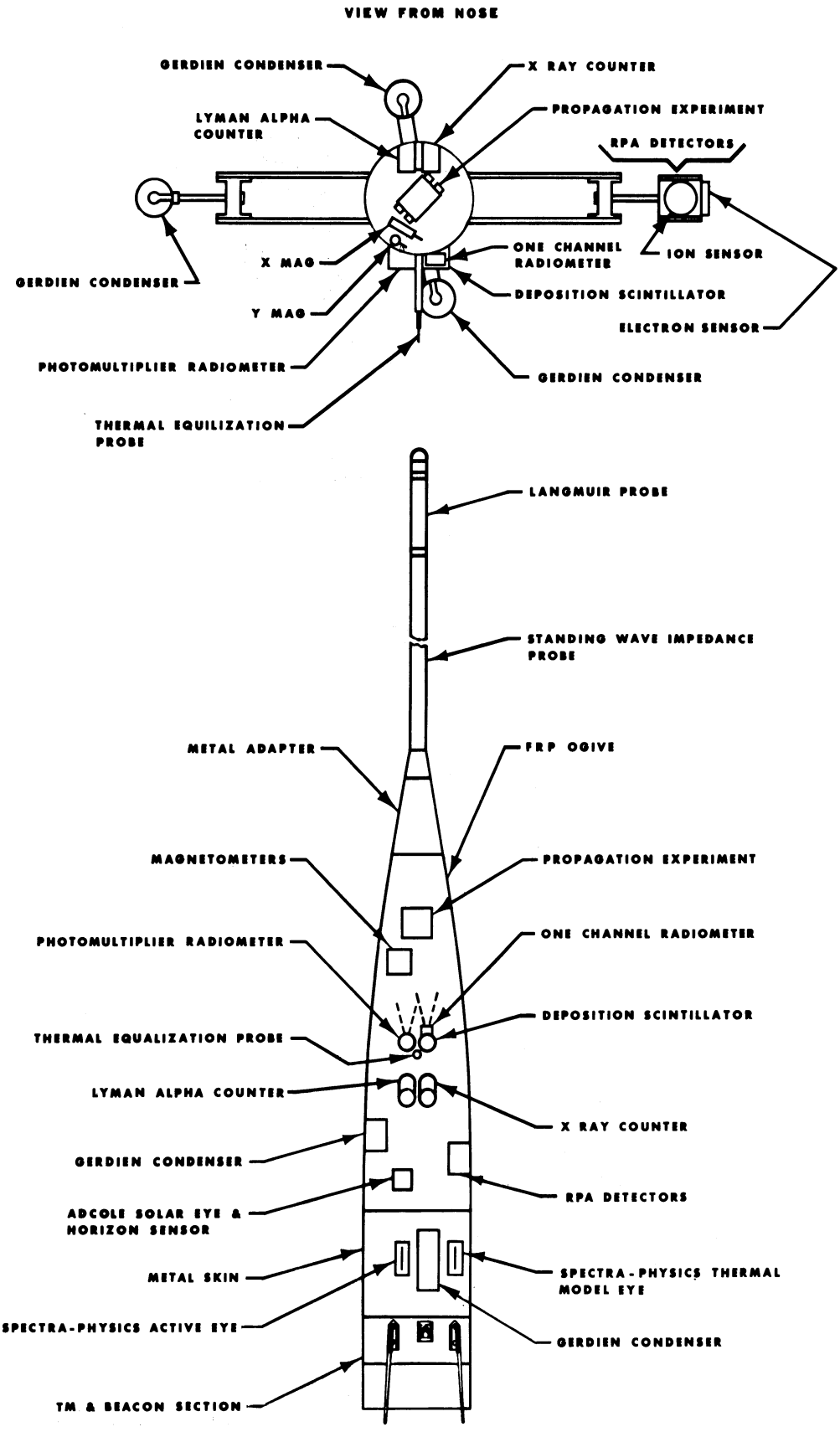

Fig. 1. Black Brant AC 17.604. Payload layout and sensor locations.

Fig. 2. Nose tip Langmuir probe system completely assembled.

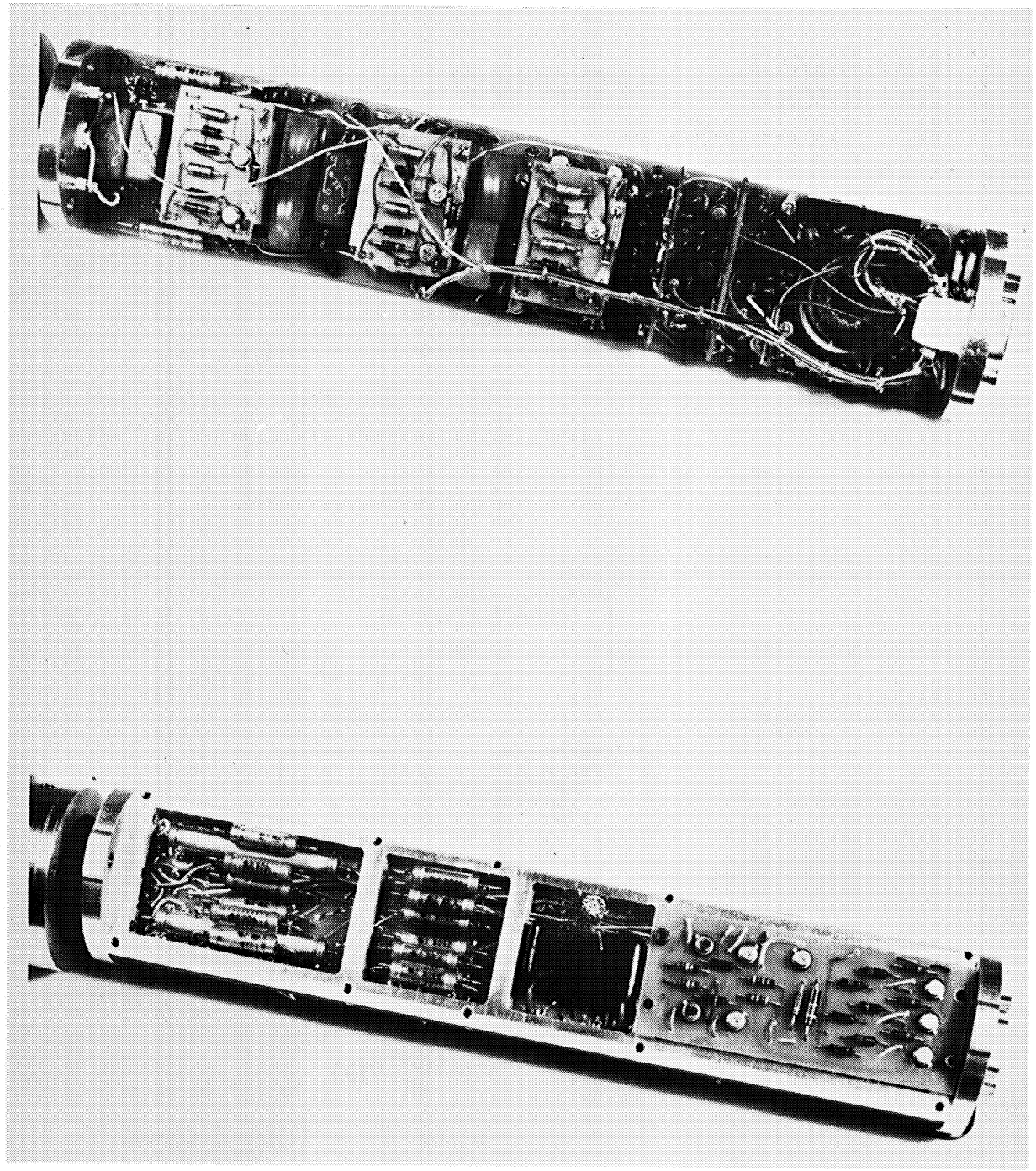

Fig. 3. Front and back view of the Langmuir probe system electronics with housing removed.

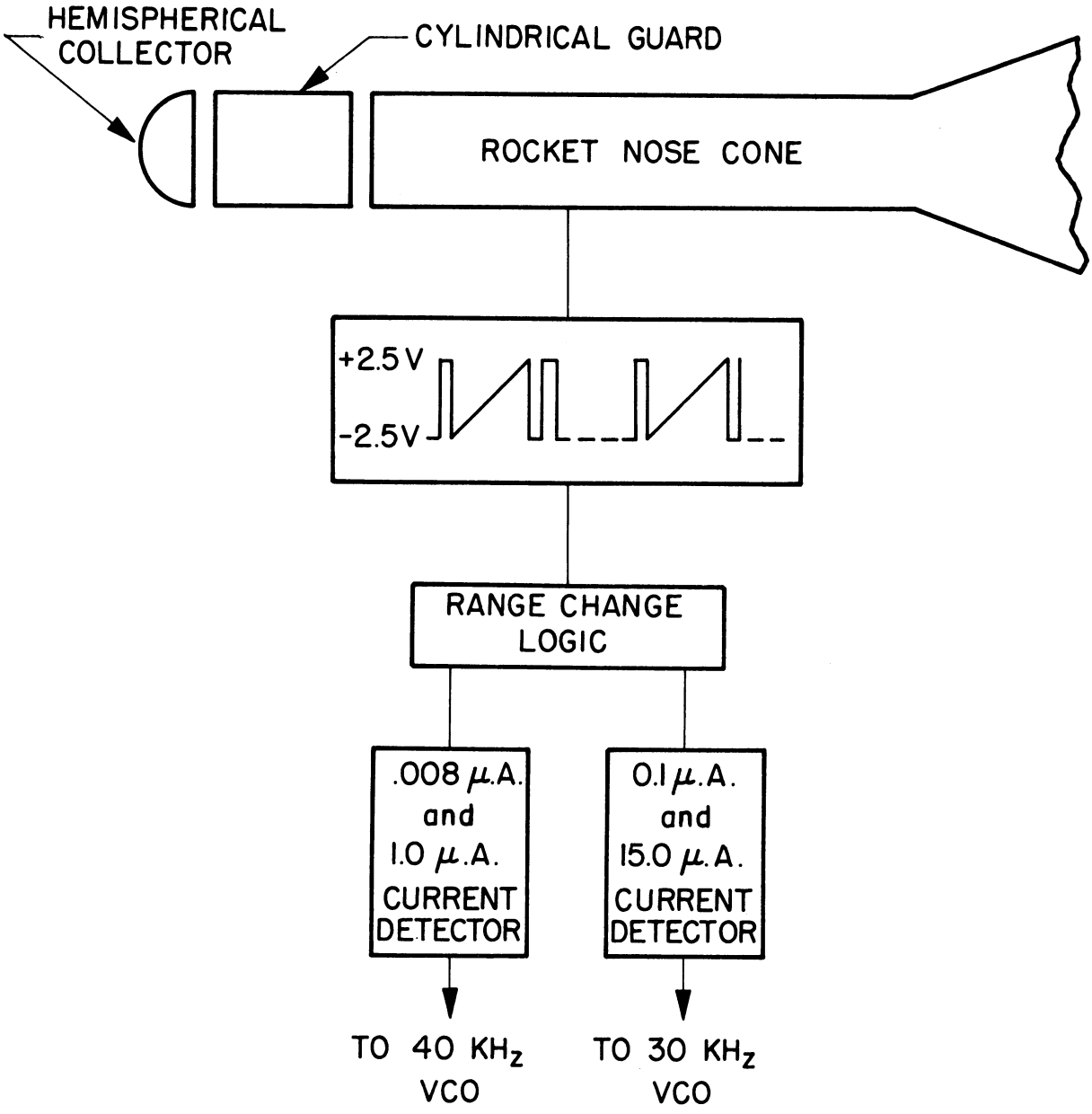

Fig. 4. Simplified Langmuir probe system block diagram.

in Fig. 5 while Fig. 6 shows the interface connections to the FM-FM telemetry system and power supply aboard the rocket. As usual, the rocket body serves as the voltage reference to the entire system.

B. LANGMUIR PROBE MECHANICAL CONSTRUCTION

The solid hemispherical nose tip Langmuir probe has a diameter of 2.5 in. and was machined from 303 stainless steel. The guard ring and housing tube were made of 304 stainless steel. Ceramic insulations separate the guard ring from the nose tip and the housing tube. The entire system is attached to the rocket nose cone tube via a 303 stainless steel adaptor. Figure 7 shows the complete mechanical drawings and parts specifications; section CC shows the location of the electronic support assembly. The completed system was vibration tested for mechanical and electrical integrity prior to integration with the rest of the payload.

C. SYSTEM ELECTRONICS

The Langmuir probe electronic system schematic is shown in Fig. 8. Briefly, the probe and guard are driven by the same voltage generator with the voltage format shown in the top segment of Fig. 5. The probe current is alternately measured by the two current detectors which are characterized by the two operational amplifiers AMP1 and AMP 2 in Fig. 8. Each detector has two current ranges. The output of the 0.008 μA current range of detector 1 and the 0.1 μA current range of detector 2 are biased positively by approximately 2.5 v with respect to the system ground. AMP 3 is the operational amplifier used to generate the saw-tooth segment of the generator voltage. R_1 (25 megohms) and R_2

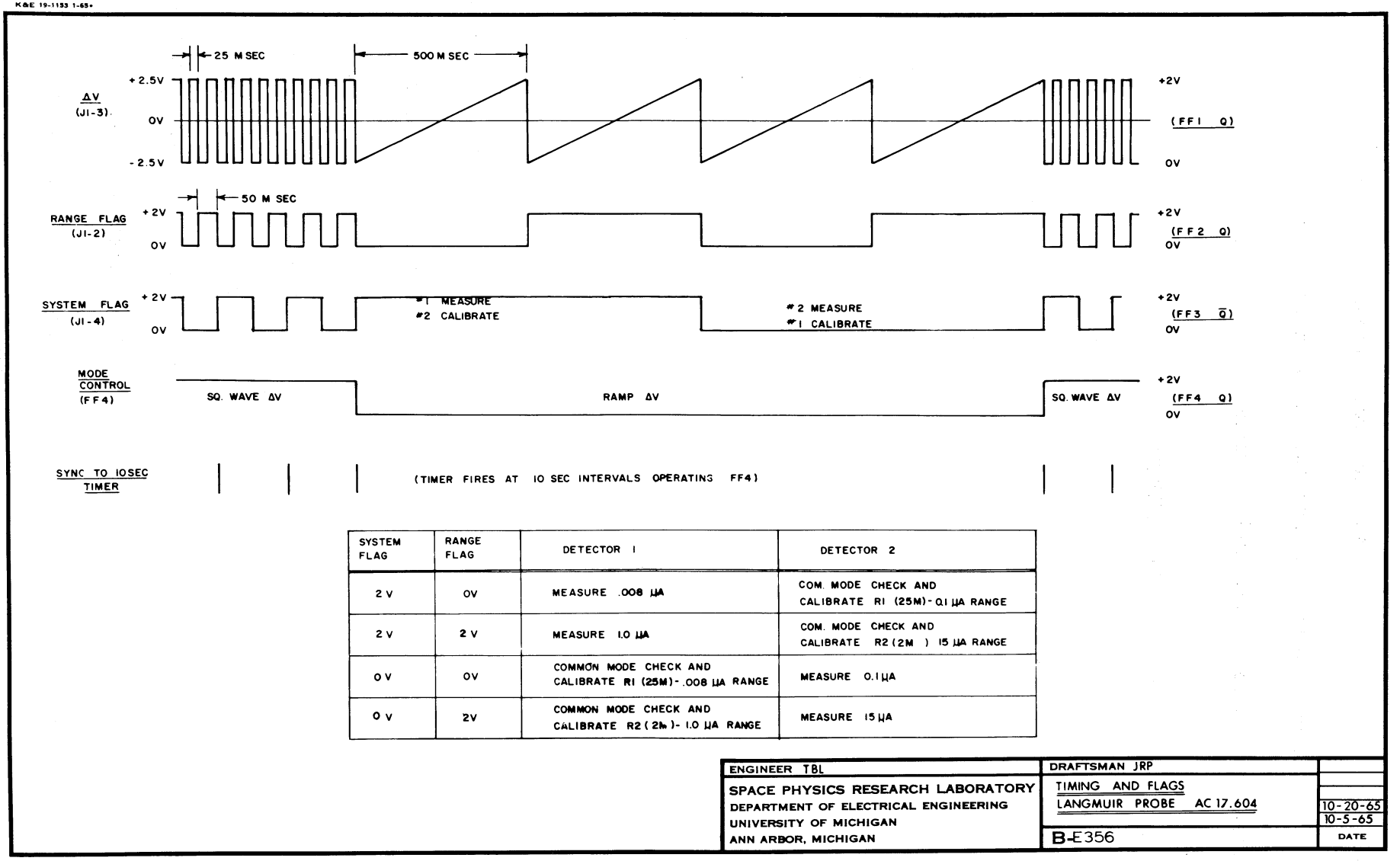

SYSTEM FLAG	RANGE FLAG	DETECTOR 1	DETECTOR 2
2 V	0V	MEASURE .008 μA	COM. MODE CHECK AND CALIBRATE R1 (25M)- 0.1 μA RANGE
2 V	2 V	MEASURE 1.0 μA	COM. MODE CHECK AND CALIBRATE R2 (2M) 15 μA RANGE
0 V	0V	COMMON MODE CHECK AND CALIBRATE R1 (25M)- .008 μA RANGE	MEASURE 0.1 μA
0 V	2V	COMMON MODE CHECK AND CALIBRATE R2 (2M)- 1.0 μA RANGE	MEASURE 15 μA

ENGINEER TBL	DRAFTSMAN JRP	
SPACE PHYSICS RESEARCH LABORATORY DEPARTMENT OF ELECTRICAL ENGINEERING UNIVERSITY OF MICHIGAN ANN ARBOR, MICHIGAN	TIMING AND FLAGS LANGMUIR PROBE AC 17.604	10-20-65 10-5-65
	B-E356	DATE

Fig. 5. System timing and flags. The top segment is the generator voltage wave form.

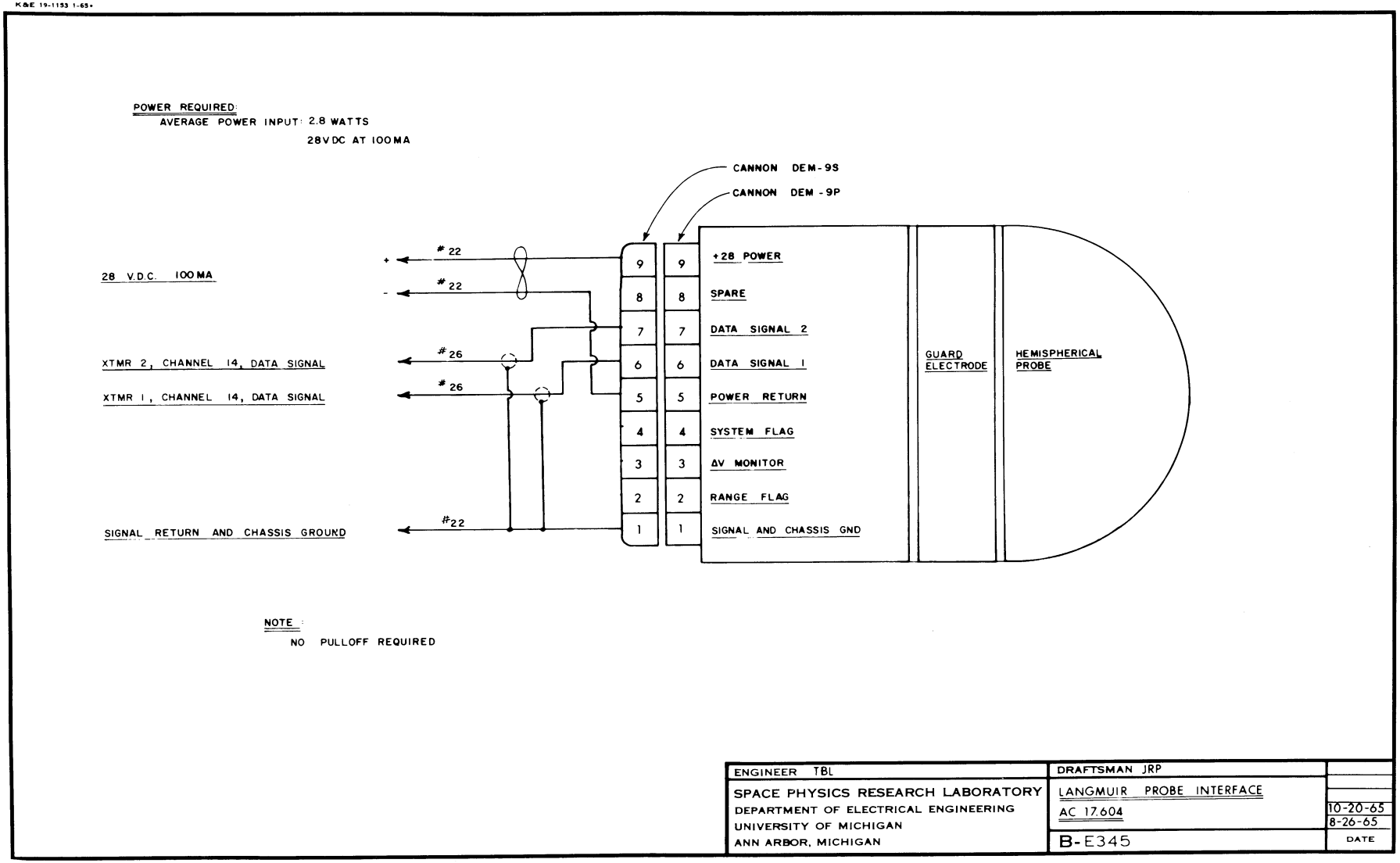

Fig. 6. System interface, showing pin connections to the rocket telemetry system and power supplies.

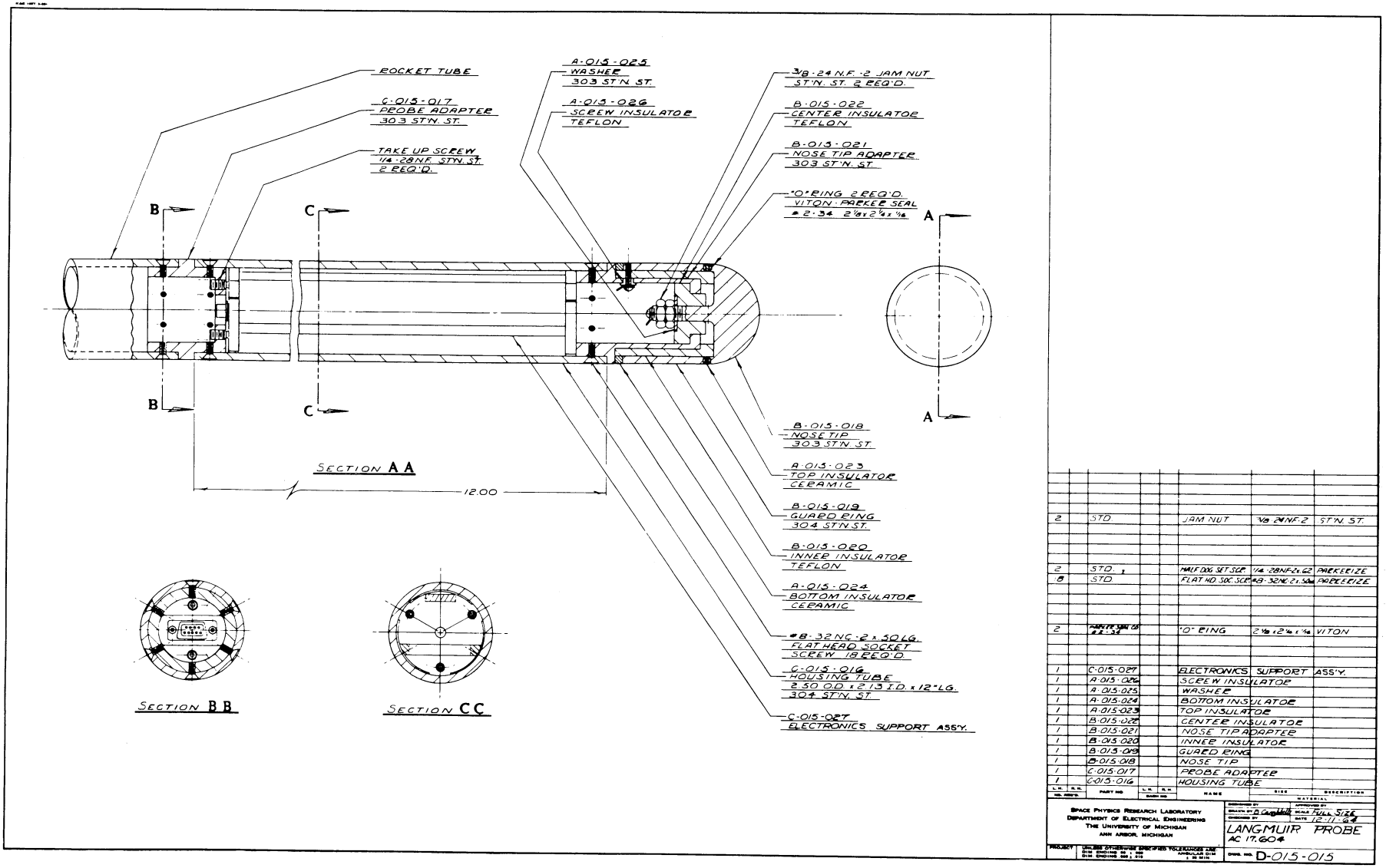

Fig. 7. Langmuir probe system mechanical drawings and parts specifications.

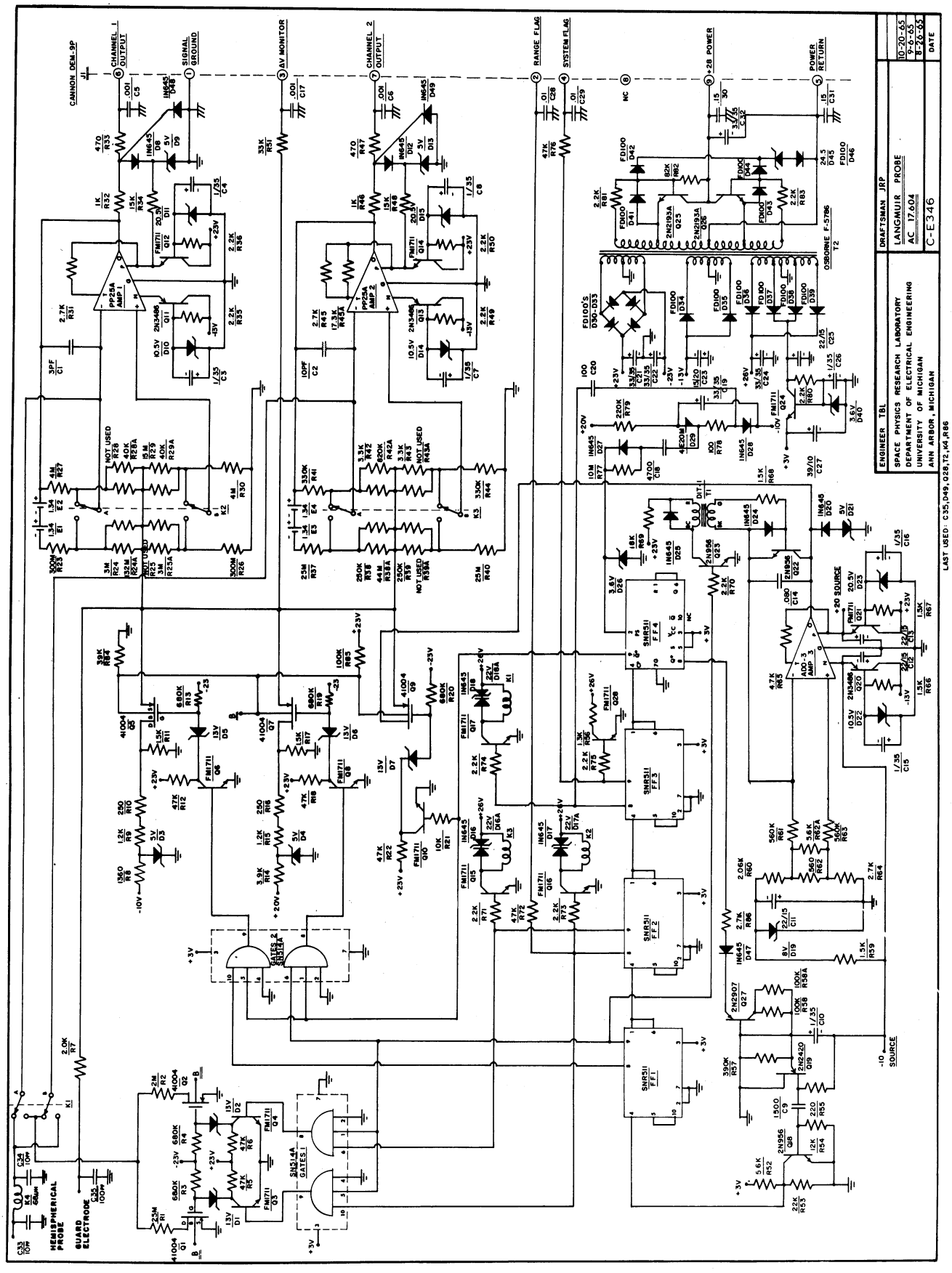

Fig. 8. Langmuir probe system electronics schematic.

(2 megohms) are the calibration resistors. The system logic made generous use of micromodules because of reliability in performance and ease of construction. The lower right hand corner section of Fig. 8 shows the system power regulator. During the calibration phase, the detector input is first shorted together to simulate zero probe current (common mode check); this is followed by applying the generator voltage successively to the two calibration resistors and measuring the resulting current. The use of operational amplifiers for sweep voltage generation and current detection enhances both reliability in performance and reduction in construction time.

D. CURRENT DETECTOR

The current detectors used in the Langmuir probe system consisted of two Philbrick PP25A operational amplifiers and four sets of matched range resistors. A single range detector schematic is shown in Fig. 9. The resistance pairs designated R_1 and R_2 are separately matched to 0.1% and track each other to within 25 parts per million (ppm) over the expected temperature range of -25°C to +50°C.

For purposes of analysis, the Langmuir probe is represented by an equivalent resistance R_p. The open loop gain of the amplifiers has a value greater than 20,000, and an input impedance of about 10^{12} ohms. For all practical purposes, the current flowing into terminals (1) and (2) are zero and so we can write the following equations:

$$e_1 - e_2 = -\frac{E_o}{A} \qquad (1)$$

$$i_1 = i_f + i_p \qquad (2)$$

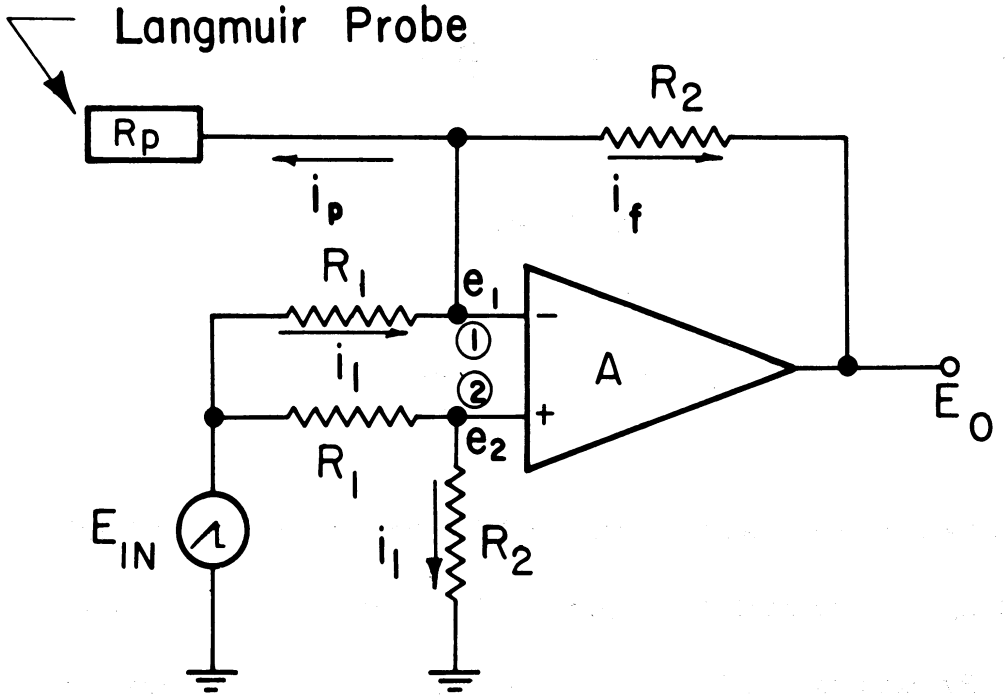

Fig. 9. Single range current detector schematic.

$$i_f = \frac{e_1 - E_o}{R_2} \tag{3}$$

$$i_p = \frac{e_1}{R_p} \tag{4}$$

$$e_1 = E_{in} - i_1 R_1 \tag{5}$$

$$e_2 = E_{in} \frac{R_2}{R_1 + R_2} \tag{6}$$

Substituting for the numerical value of A (the open loop gain) into Eq. (1) we find that E_o/A is negligible compared with either e_1 or e_2, and so we get $e_1 \simeq e_2$. By eliminating i_1, i_f, i_p, e_1, and e_2 from the above equations we get the final result:

$$E_o = E_{in} \left(\frac{R_2}{R_1 + R_2} \right) \frac{R_2}{R_p} \quad . \tag{7}$$

Since e_1 and e_2 are equal we may substitute Eq. (6) for e_1, in Eq. (4) and use the result in Eq. (7) to give:

$$E_o = R_2 i_p \quad . \tag{8}$$

The last equation shows that the detector output voltage is directly proportional to the probe current with R_2 the proportionality factor. Therefore, different current ranges are obtained by changing the value of R_2. From the overall performance of the detector, it was found that range change is best accomplished by changing the resistors R_1 along with R_2, but keeping the resistance ratio R_2/R_1 constant. In order to achieve a high signal to noise

ratio and adequate common mode rejection, the optimum value for the ratio R_2 to R_1 was found to be 100 for this particular design configuration.

E. SWEEP VOLTAGE GENERATOR

The sweep voltage generator employed a Fairchild ADO-3 operational amplifier and a low leakage silver-dip-mica capacitor. The schmatic for the generator is shown in Fig. 10. R_1 and R_2 serve as a voltage divider and set the starting level of each sweep. Following the general analysis method of the previous section we get the following relation:

$$e_o = e_2 + \frac{1}{RC} \int (e_g - e_2)dt \ . \qquad (9)$$

The system logic and timing determines the period of each sweep and the slope of the ramp is determined by the RC product. In practice the available space dictates the value of C, so that any slope change is best accomplished by varying the resistor R as was done in the present system.

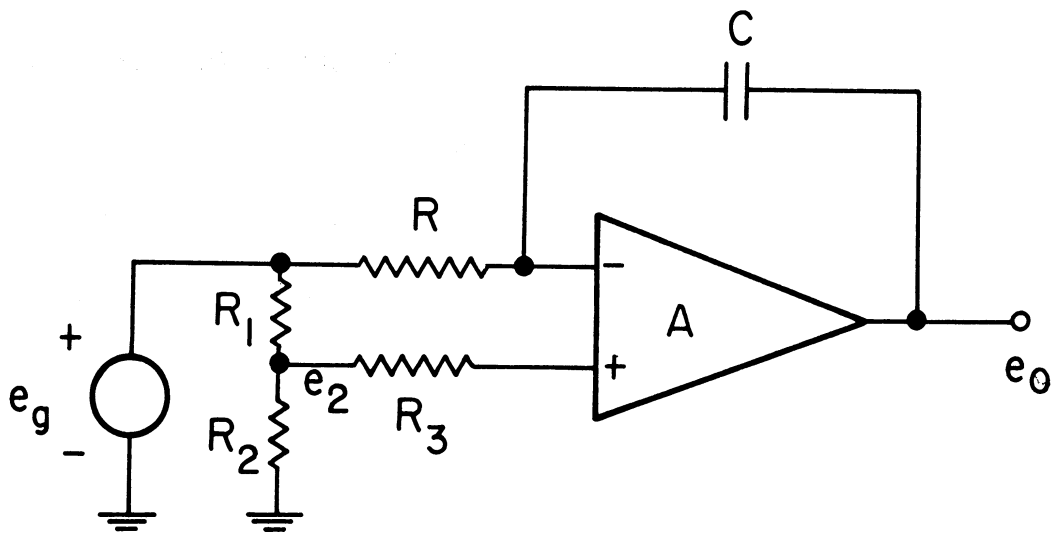

Fig. 10. Sweep voltage generator schematic.

III. THEORETICAL BACKGROUND

A. REVIEW OF PROBE THEORY IN THE LOWER IONOSPHERE

The theory of electrostatic probes carried by supersonic rockets in the D- and lower E-regions of the ionosphere, where the neutral particle density is high, has not been developed adequately enough for any practical application. Pearl[2] conducted an extensive review of the work done in this area, but found no satisfactory theory applicable to a moving spherical Langmuir probe. He further concluded that it is unlikely that an analytic solution of the problem can be obtained in the near future. He then attempted to solve the problem of a hemispherical probe moving at supersonic speeds by a numerical method. Unfortunately there was no tangible conclusion, nor specific results that can apply to an actual experiment in the D-region of the ionosphere. Smith[3] avoids this difficulty by using electron density values from propagation experiments to calibrate the probe current to his Langmuir probe in terms of ambient electron density. This method appears reliable, provided the effects of vehicle speed and other dynamic parameters, which affect the probe current, are properly accounted for. Balmain[4] considered a spherical probe at high pressures, assuming the probe to be stationary. He suggests that the effects of vehicle speed can be overcome by operating the probe at high negative voltages. The Langmuir probe system described in this report has a potential of ±2.5 v with respect to the rocket body, and therefore Balmain's conditions are not met. In a very recent article, Su and Sonin[5] considered the case of a moderately ionized gas, but here again the condition of a stationary probe renders this

work inapplicable to the present system.

B. GENERAL ION CURRENT EQUATION

In view of the lack of an adequate working theory which is applicable in the D- and lower E-regions of the ionosphere, the authors adopted an empirical procedure by using various collisionless theories that are directly applicable only to the upper portions of this flight, but which are being used for reducing the data for all the region above 80 km. The collisionless theory of moving spherical collectors has been discussed by various authors (Medicus,[6] Kanal,[7] Sagalyn et al.,[8] Nagy et al.,[9] and Laframboise[10]). They derived the current collection characteristics of such moving probes by making a number of simplifying assumptions. The assumptions made by Kanal were as follows:

1. The sheath surrounding the moving spherical collector remains spherical;
2. The velocity distribution of the ambient particles is Maxwellian;
3. Electrons and positive ions are present in equal numbers;
4. The mean free path of the particles is large compared to the dimensions of the collector and the sheath; and
5. All ions reaching the collector are collected.

A discussion of the above assumptions as related to our experiment will be given later. For now we present the equation of the general ion current to a moving spherical collector as given by Kanal[7]:

$$I_i = J_{io} A \left[\left(\frac{a}{r} \right)^2 F(x) - \frac{a^2 - r^2}{r^2} H(\gamma \eta^{1/2}, x) \right] \qquad (10)$$

where

$$F(x) = \frac{\sqrt{\pi}}{2x}\left(x^2 + \frac{1}{2}\right)\mathrm{erf}(x) + \frac{1}{2}\exp(-x^2)$$

$$-2H(\gamma\eta^{1/2},x) = \frac{\sqrt{\pi}}{2x}\left(\gamma^2\eta - x^2 - \frac{1}{2}\right)\left\{\mathrm{erf}(\gamma\eta^{1/2}+x) - \mathrm{erf}(\gamma\eta^{1/2}-x)\right\}$$

$$+ \frac{(\gamma\eta^{1/2}-x)}{2x}\exp\left\{-(\gamma\eta^{1/2}+x)^2\right\} - \frac{(\gamma\eta^{1/2}+x)}{2x}\exp\left\{-(\gamma\eta^{1/2}-x)^2\right\}$$

$\gamma^2 = \dfrac{r^2}{a^2-r^2}$

a = sheath radius

r = collector radius

$\eta = \dfrac{qV}{kT}$

A = collector area

$J_{io} = qN_i\sqrt{kT_i/2\pi m_i}$ is the random ion current density

$x = \dfrac{w}{c_o}\dfrac{2}{\sqrt{\pi}}$

$c_o = \sqrt{8kT_i/\pi m_i}$ is the average thermal speed of the ions

w = vehicle or probe speed

V = probe potential with respect to the ambient ionosphere

T_i = ion temperature

m_i = mean ion mass

k = Boltzmann's constant

q = electronic charge

N_i = ion number density

The limits of $F(x)$ and $H(\gamma\eta^{1/2},x)$ as $x \to 0$ are given by Eqs. (11) and (12), respectively;

$$\lim_{x \to 0} F(x) = 1 \tag{11}$$

$$\lim_{x \to 0} H(\gamma \eta^{1/2}, x) = e^{-\gamma^2 \eta} . \tag{12}$$

Substituting the results of Eqs. (11) and (12) into Eq. (10), the classical Langmuir[11] equation for a stationary probe is obtained:

$$\lim_{x \to 0} I_i = J_{io} A \left[\left(\frac{a}{r} \right)^2 - \frac{a^2 - r^2}{r^2} \exp(-\gamma^2 \eta) \right] . \tag{13}$$

Using the following typical daytime E-region parameters (T_i = 300°K, m_i = 30) and taking the probe to be at -4 v with respect to the ambient ionosphere a value of 154 is obtained for η. Since a is comparable in magnitude to r, we conclude that for the values of x encountered in flight, the second term in Eq. (10) is negligible compared to the first term, and so we can write

$$I_i \cong J_{io} A \left(\frac{a}{r} \right)^2 F(x) . \tag{14}$$

The effect of the probe motion is accounted for by the term F(x) which is plotted in Fig. 11.

C. SHEATH MODEL

In order to calculate the ion density from Eq. (14) one needs to know the relationship between the sheath radius and the probe potential. For the condition when the dimension of the probe is much greater than the sheath thickness Bettinger and Walker[12] obtained the following relations

$$s_1 = \left(\frac{2}{3} \right)^{1/4} h \eta^{3/4} . \tag{15}$$

The above form was also derived by Hoegy and Brace[13] with a somewhat different

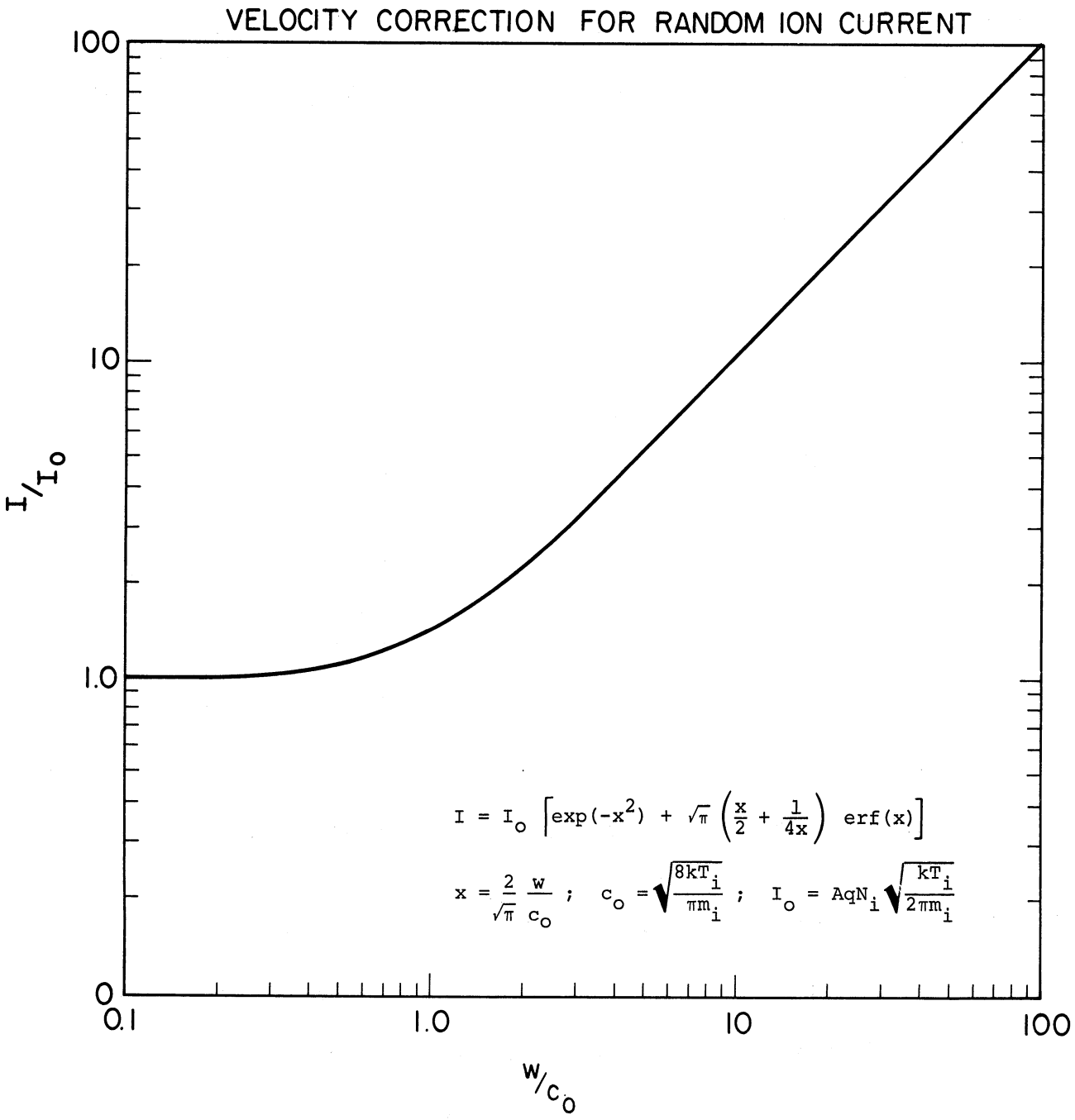

Fig. 11. Effects of probe velocity on the random ion current to a moving spherical Langmuir probe.

coefficient. Bettinger and Walker[12] obtained the following relationship for the case when the sheath thickness is much greater than the radius of the collector.

$$s_2 = 0.83 \left(\frac{r}{h}\right)^{1/3} h\eta^{1/2} \qquad (16)$$

where

s = a-r is the sheath thickness

$h = \sqrt{\epsilon_o kT/q^2N} = 68.6\sqrt{T/N}$ is the Debye length

Figure 12 is a graphical comparison of Eqs. (15) and (16) for $N = 3x10^{11}$ particles per cubic meter and $T_i = 300°K$. The radius of the probe r, is 3.17 cm. From Fig. 12 at 4 v s_1 is 8.6 cm thus contradicting the requirement that $s_1 \ll r$. The requirement that s_2 be much greater than r is partially met. s_2 was chosen as the appropriate sheath model for reasons to be discussed later.

D. ION CURRENT EQUATION FOR DENSITY CALCULATIONS

In the previous section we adopted s_2 as the most appropriate sheath model. This sheath relation will be used in the rest of this report, so the subscript will be dropped from now on to simplify the notation. We defined, s = a-r, therefore, $\frac{a}{r} = \frac{s}{r} + 1$. Substituting this to Eq. (14) we get:

$$I_i = J_{io} A \left(\frac{s}{r} + 1\right)^2 F(x) . \qquad (17)$$

Employing the definition of h, J_{io} and the sheath model from Eq. (16) we can write:

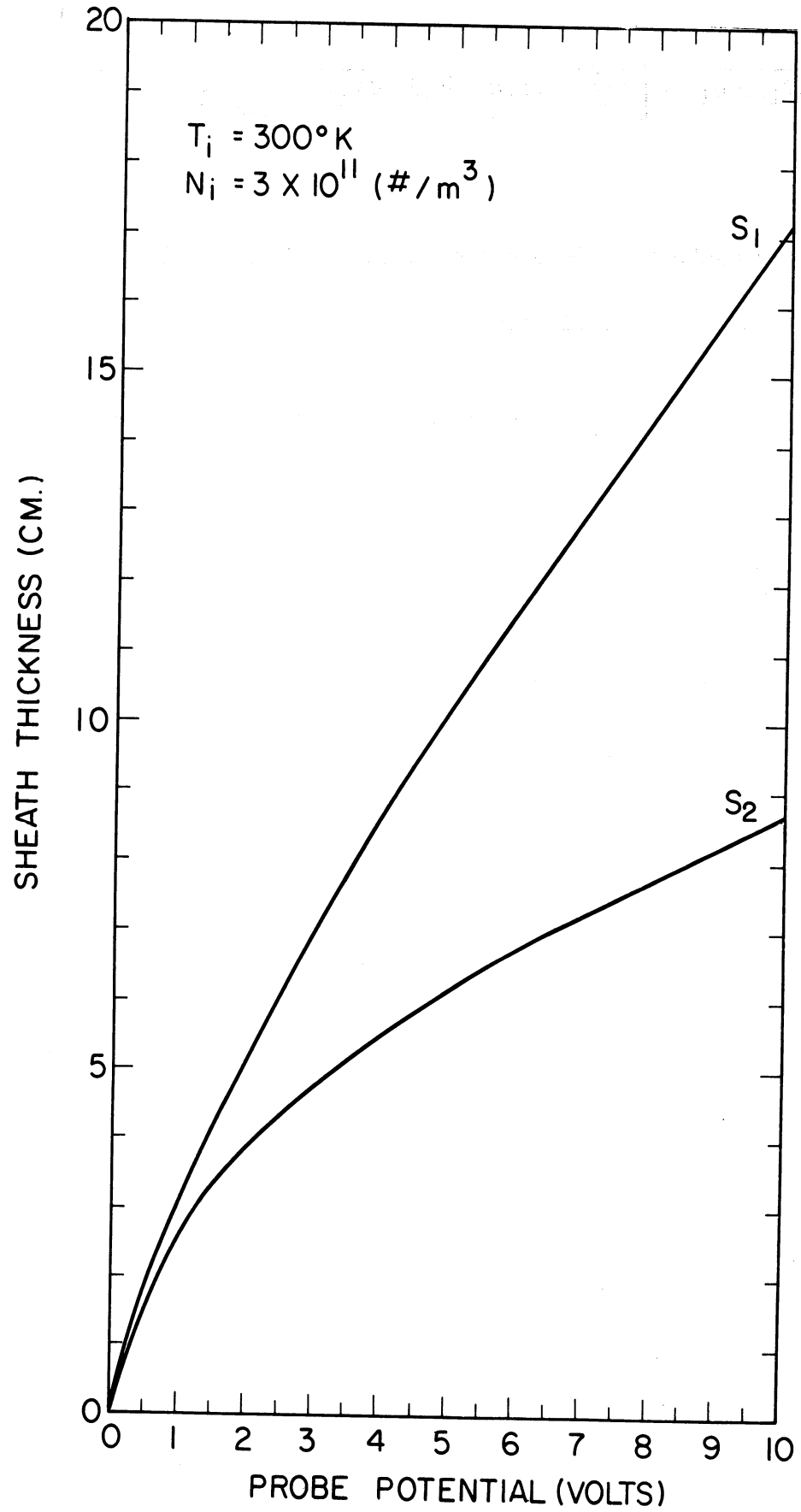

Fig. 12. Graphical illustration of sheath thickness as a function of probe potentials for the two sheath models s_1 and s_2.

$$I_i = qA\sqrt{kT_i/2\pi m_i}\, N_i \left[\frac{0.83}{r}\,\eta^{1/2}\,68.6\,\sqrt{T_i/N_i}\left(\frac{r}{68.6}\sqrt{N_i/T_i}\right)^{1/3} + 1\right]^2 F(x) \,. \tag{18}$$

Introducing new symbols to denote the constants in Eq. (18) we obtain the ion current equation in its final form:

$$I_i = \alpha N_i [1 + \beta N_i^{-1/3}]^2 F(x) \tag{19}$$

where

$$\alpha = qA\sqrt{kT_i/2\pi m_i}$$

$$\beta = 0.83\eta^{1/2}/r^{2/3}\,(\epsilon_o kT_i/q^2)^{1/3} \,.$$

IV. DATA REDUCTION AND RESULTS

A. FLIGHT INFORMATION AND TELEMETRY DATA

The Langmuir probe system was launched at 12:16 PM CST on September 28, 1966 aboard Black Brant AC 17.604. The rocket reached an altitude of about 116 km. The system utilized two VCO channels operating at 30 KHz and 40 KHz as outlined in Section II-A. The entire system operated satifactorily after take-off; however, when the 30-in. boom and the radiometer doors were ejected, the signal from the 40 KHz channel became extremely noisy and intermittent. Common to both channels was a square wave modulation of the detector output with a period of 200 ms, which corresponds to the switching time of the standing wave impedance probe experiment. It was determined that this modulation was due to changes in the rocket equilibrium potential when the standing wave impedance probe switched from 3 MHz to 7 MHz at 100-ms intervals. The net result of the loss of data from the 40 KHz channel means that the 0.008 μA and 1.0 μA detectors provided no useful data. This is particularly unfortunate since reliable electron temperature information is contained in the 1.0 μA range detector. As it turns out from the data available, that this range also would have provided the most reliable ion current information for the entire flight with the exception of a 15-km interval centering around the 100-km level. This is because the 0.1 μA range suffered ion current saturation while the 15 μA range had poor resolution in the lower altitudes. The ion current saturation in the 0.1 μA range detector also introduces errors in the electron temperature derived from its output. The combination of telemetry interference

and ion current saturation resulted in only four electron temperature values being obtained, and even these the authors consider to be questionable. Figure 13 is a section of the telemetry data corresponding to the altitude of 109.5 km.

In most circumstances the electron current is used to deduce the ambient charged particle density, because it is much less sensitive to probe orientation and velocity than the ion current, and also no assumption on the ion composition is needed. However, in this particular flight, the positive voltage of 2.5 v with respect to the rocket skin was not sufficient to drive the probe into the electron accelerating mode. Nagy[14] reported this to be due to the fact that the rocket body somehow assumed a more negative potential than anticipated. The net result is that only positive ion saturation current, at -2.5 v with respect to the rocket skin, was measured. Figure 14 shows the average ion current as a function of altitude and the horizontal bars represent twice the standard deviation for the upleg data points. Because of increasing angle of attack past the apogee, the interpretation of downleg ion current in terms of positive ion density becomes very difficult; therefore, the downleg ion density is likely to contain significant errors.

B. ION DENSITY CALCULATIONS

This section describes the calculation of ion density from measured ion current utilizing Eq. (19) and the velocity correction of random ion current from Fig. 11. The procedure of ion density reduction is given below.

1. The measured ion current was first corrected for probe velocity effects using Eq. (19) and Fig. 11. This was done by recording the

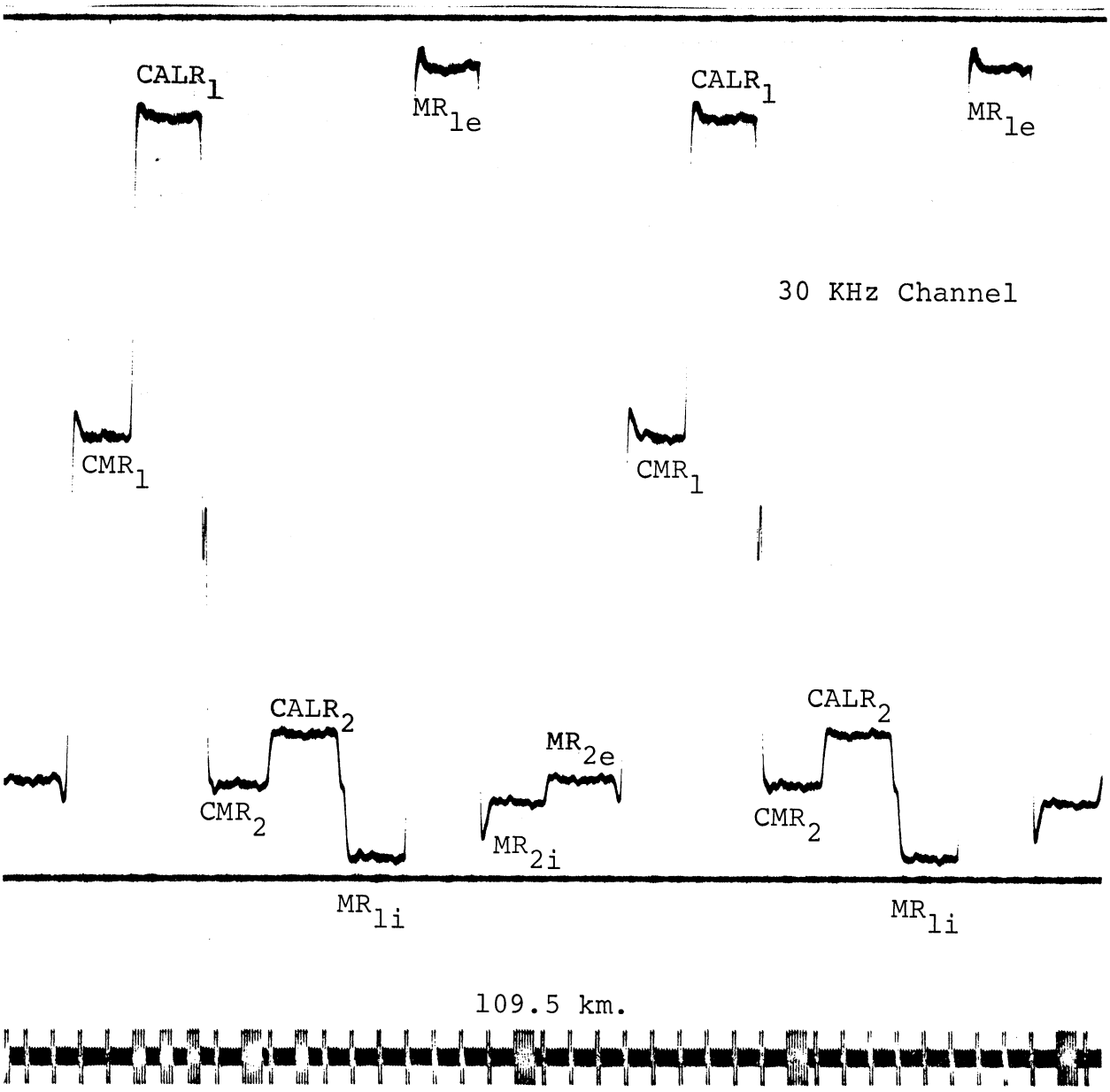

0.1 μA:	Range 1;	15 μA: Range 2
CMR_1:	Range 1	common mode check
CMR_2:	Range 2	common mode check
$CALR_1$:	Range 1	calibration
$CALR_2$:	Range 2	calibration
MR_{1i}:	Range 1	ion current measurement
MR_{2i}:	Range 2	ion current measurement
MR_{1e}:	Range 1	electron current measurement
MR_{2e}:	Range 2	electron current measurement

Fig. 13. Section of Langmuir probe telemetry data.

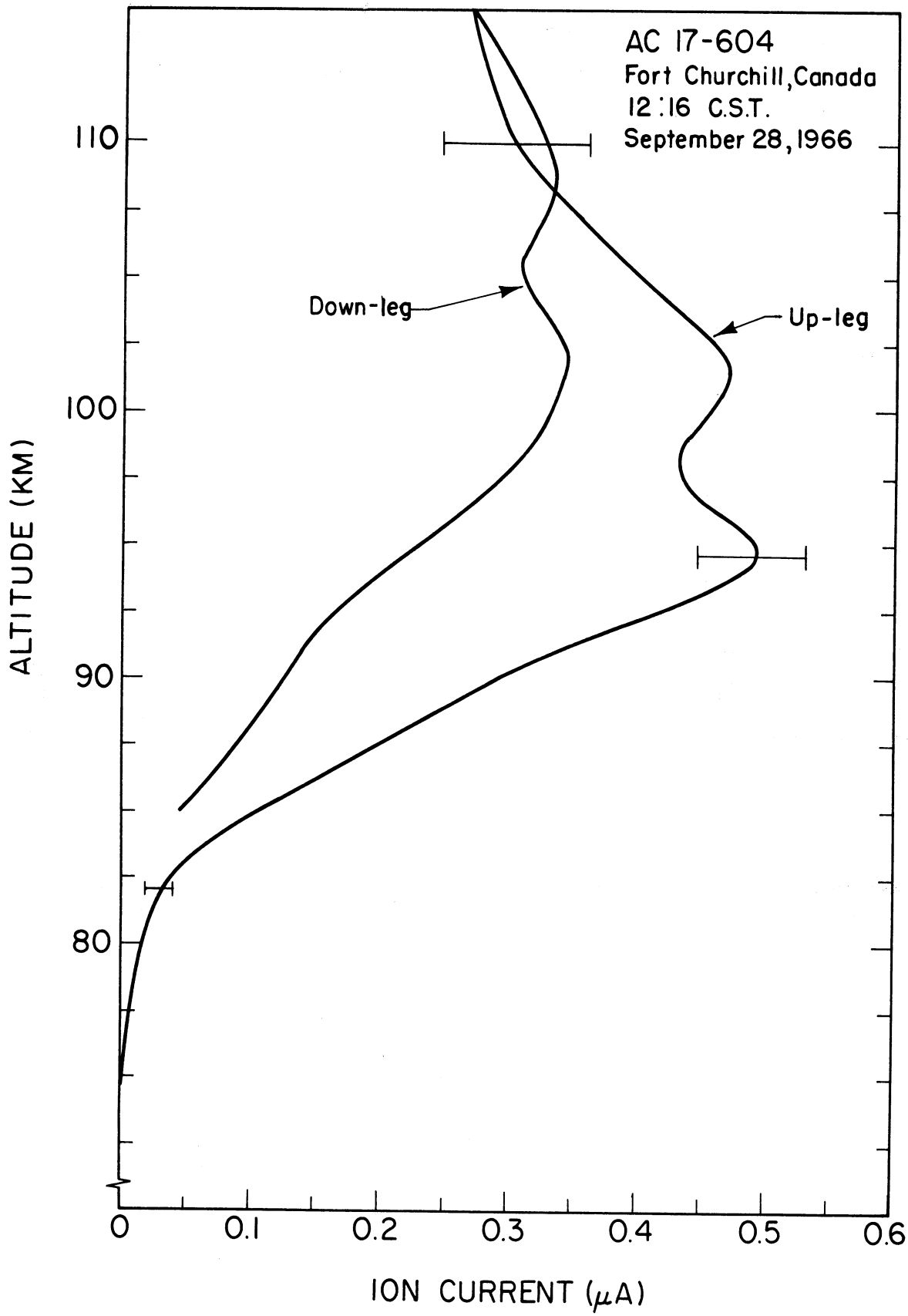

Fig. 14. Average of measured ion current to the hemisphereical Langmuir probe vs. altitude.

value of I/I_o for specified values of x and then dividing the measured ion current by this ratio to give an "expected true" ion current. This corresponds to dividing Eq. (19) by F(x).

2. Using the "expected true" ion current (measured ion current corrected for probe velocity effects) and denoted by I_{it}, and Eq. (19 we get:

$$I_{it} = \alpha N_i [1 + \beta N_i^{-1/3}]^2 . \qquad (20)$$

The ion density was calculated by an iterative method. We first assume an ion density and evaluate the right hand side of Eq. (20). The result is compared with I_{it} and the value of the ion density N_i was considered acceptable when the two sides of Eq. (20) agree to within 1.0%.

The ion temperature in the region 85-115 km is expected to be the same as the neutral particle temperature. Using the information given in the CIRA 1965 Model Atmosphere, 300°K was selected as an appropriate average value for the ion temperature, and was used throughout all the calculations. An ion mass of 30 was chosen for this region following the ion composition measurements of Narcisi and Bailey[15] who reported the predominance of ions of mass 30^+ and 32^+ above 82 km. Using the chosen ion temperature of 300°K and mean ion mass of 30, we get $\alpha = 1.161 \times 10^{-19}$ and $\beta = 1.155 \times 10^4$. Here we have taken the probe voltage to be -4 v with respect to the ambient ionosphere. This choice is supported by the rocket equilibrium potential measurements of Bettinger* employing the Hot Probe and Ulwick* using the Ion Trap, which showed that the vehicle

*Private communications.

potential fluctuated about an average of -1.5 v with respect to the ambient ionosphere. For ion current measurement, the Langmuir probe potential was at -2.5 v with respect to the rocket. Therefore, the Langmuir probe potential is -4 v with respect to the ambient ionosphere. Table I shows the measured and expected true ion current and final ion density as a function of altitude. Figure 15 is a plot of ion density vs. altitude. Figure 16 is a comparison with the preliminary electron density profile obtained by Bowhill* from the CW Propagation experiment, and the electron density profile obtained by Ulwick et al.,[16] with the standing wave impedance probe (SWIP). Note the change in density scale with reference to the Langmuir probe profile; this separation of the curves affords a better comparison of the three density results.

C. ELECTRON TEMPERATURE

As indicated in Section IV-A, the available data provided very little information from which to determine the electron temperature. However, it was found that electron temperature reduction was possible from four probe characteristics. Reduction of the electron temperature follows the standard method by extrapolating the ion current and subtracting this from the total current. The resulting portion is the electron current. In the retarding region the electron current is governed by Eq. (21)

$$I_e = I_{eo} \exp\left(-\frac{qV}{kT_e}\right). \tag{21}$$

The electron temperature T_e is therefore given by:

$$T_e = \frac{q}{k} \frac{(V_2-V_1)}{\ln(I_2/I_1)}. \tag{22}$$

*Private communications.

TABLE I

LANGMUIR PROBE ION CURRENT, POSITIVE ION DENSITY VS. ALTITUDE
(AC 17.604)

Alt. (km)	I_i Up	I_i Down	I_{it} Up	I_{it} Down	N_i Up	N_i Down
76	0.004		0.00179		1.45×10^{6}	
78	0.008		0.00376		1.29×10^{7}	
80	0.015		0.00711		8.95×10^{7}	
82	0.030		0.0146		5.55×10^{8}	
84	0.072		0.0360		5.47×10^{9}	
86	0.142	0.078	0.0736	0.0404	2.75×10^{10}	7×10^{9}
88	0.215	0.098	0.1120	0.0510	6.45×10^{10}	1.2×10^{10}
90	0.290	0.125	0.1576	0.0679	1.22×10^{11}	2.26×10^{10}
92	0.390	0.155	0.2179	0.0866	2.21×10^{11}	3.77×10^{10}
94	0.480	0.202	0.2759	0.1161	3.32×10^{11}	6.80×10^{10}
96	0.442	0.255	0.2600	0.1500	3.02×10^{11}	1.15×10^{11}
98	0.432	0.303	0.2650	0.1859	3.12×10^{11}	1.67×10^{11}
100	0.455	0.332	0.2862	0.2088	3.55×10^{11}	2.06×10^{11}
102	0.467	0.345	0.3072	0.2270	4.05×10^{11}	2.40×10^{11}
104	0.425	0.323	0.2872	0.2182	3.59×10^{11}	2.21×10^{11}
106	0.380	0.312	0.2714	0.2229	3.26×10^{11}	2.3×10^{11}
108	0.340	0.333	0.2500	0.2449	2.82×10^{11}	2.74×10^{11}
110	0.305	0.328	0.2383	0.2563	2.60×10^{11}	2.96×10^{11}
112	0.286	0.310	0.2383	0.2583	2.69×10^{11}	3.00×10^{11}
114	0.274	0.285	0.2425	0.2522	2.67×10^{11}	2.87×10^{11}
115	0.270	0.270	0.2512	0.2512	2.85×10^{11}	2.85×10^{11}

I_i = measured ion current (μA).
I_{it} = ion current corrected for velocity effects (μA).
N_i = number of ions per cubic meter.

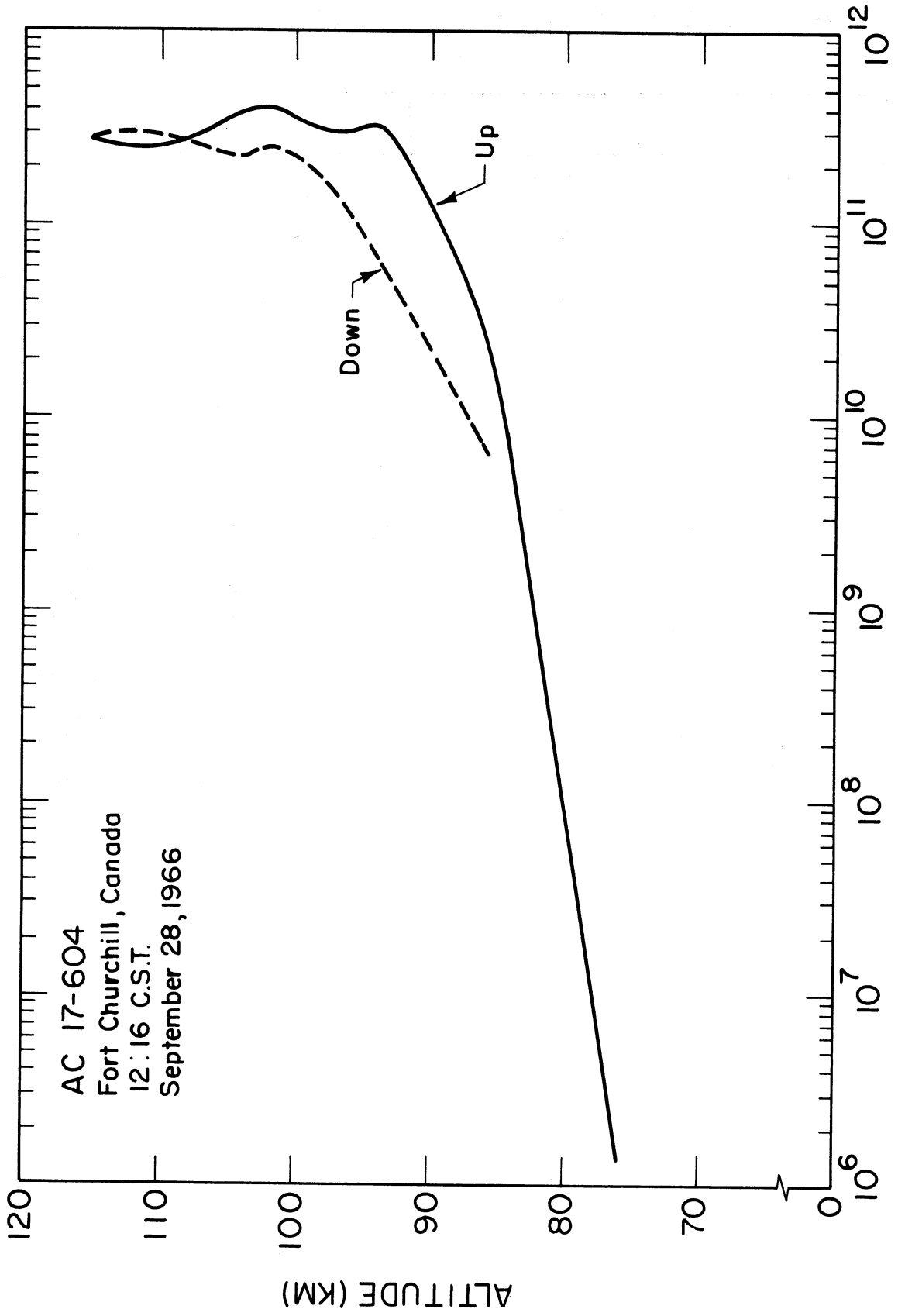

Fig. 15. Final positive ion density vs. altitude.

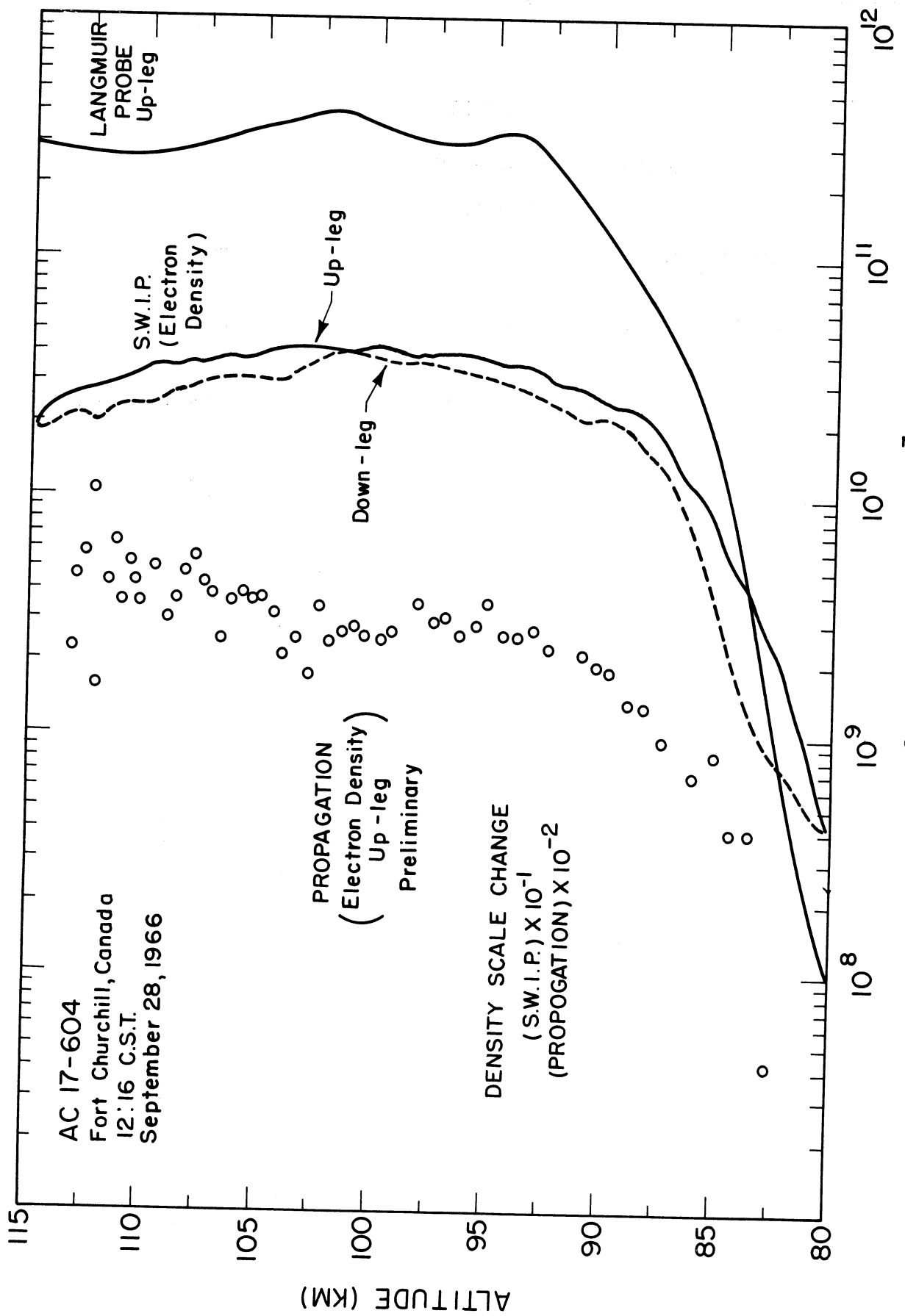

Fig. 16. Comparison of charged particle density results.

The four electron temperatures are listed in Table II

TABLE II

ELECTRON TEMPERATURE VS. ALTITUDE

(AC 17.604)

Altitude (km)	109	105	100.3	94.5
Temperature (°K)	1007	1226	1553	1510

The above values compare favorably with the electron temperatures obtained by Ulwick et al.[16]

V. DISCUSSIONS AND CONCLUSIONS

The result of the ion density calculation depends on the proper choice of a sheath model for the hemispherical Langmuir probe. At -4 v the sheath thickness s_1 is greater than the probe radius; this clearly violates the assumption for this model which requires that r be much greater than a. On the other hand, at -4 v s_2 partially meets the requirement that a be much greater than r. The final ion density using s_2 as the sheath model, shows general agreement with the electron density profile from the Standing Wave Impedance Probe and the CW Propagation experiment above about 90 km. This indicates that s_2 is the more appropriate sheath model for the hemispherical Langmuir probe described in this report.

The region of applicability of the collisionless theory and the assumptions made by Kanal to obtain his equations will now be briefly discussed. The assumption of a spherical sheath for a sphere moving at supersonic speeds in a medium of relatively high neutral particle density is certainly questionable for the general case; however, the sheath distortion around a moving hemisphere should not be too severe for small angles of attack. Assumptions (2) and (3) given in Section III-B are believed to be satisfied at altitudes above about 85-90 km. The most significant assumption which establishes the low altitude limit for the equations used is the requirement that the mean free path be large compared to the sheath dimension. The mean free path (L) in Table III is for neutral particles and was taken from the U.S. Standard Atmosphere 1962; although the ion-neutral collision frequency differs from that of the neutral-

neutral collision frequency, the latter is sufficient to provide an approximate indication of the region where the collisionless theory is applicable. The variation of the sheath dimension is also given in Table III, and it shows that the sheath is about the same length as the mean free path around 96 km. Shulz and Brown[17] used the criterion of "ten collisions" in the sheath for a collision dominated probe; this condition occurs just above 85 km. Table III further shows that above 100 km the collisionless theory is applicable. It seems therefore the equations obtained from the collisionless theory could be used down to about 95 km.

TABLE III

POSITIVE ION DENSITY, SHEATH THICKNESS, SHEATH RADIUS, AND MEAN FREE PATH VS. ALTITUDE

Alt. (km)	N_i (#/m³)	s(cm)	a(cm)	L(cm)	L/a
80	$9x7\ x10^{7}$	80.0	83.17	0.407	0.0049
85	$1.44x10^{10}$	15.1	18.27	1.201	0.0657
90	$1.23x10^{11}$	7.4	10.57	2.563	0.242
95	$3.40x10^{11}$	5.27	8.44	6.705	0.794
100	$3.55x10^{11}$	5.19	8.36	16.29	1.950
105	$3.52x10^{11}$	5.20	8.37	38.10	4.550
110	$2.60x10^{11}$	5.76	8.93	81.5	9.130
115	$2.85x10^{11}$	5.58	8.75	171.9	19.65

The charged particle density results obtained from the various experiments were compared in Fig. 16. Above 92 km, there is reasonable general agreement; however specific differences as great as a factor of 1.5 up to about the 110-km level are present. Above 110 km the SWIP results decreased while the electron density from the propagation experiment shows an apparent increase. It is interesting to point out that the Langmuir probe ion density profile fall in

between the two electron density results above 92 km. The rapid decrease in the positive ion density below 92 km suggests the breakdown of the collisionless theory from which the results were obtained. The few electron temperature values obtained from the Langmuir probe also show reasonable agreement with those obtained by Ulwick et al.[16] We therefore believe that such a hemispherical nose tip Langmuir probe is capable of providing reliable electron temperature, electron and ion density information above about 95 km. Below this altitude the Langmuir probe can be used to obtain an indication of the charged particle density variation with altitude.

ACKNOWLEDGMENTS

The authors wish to extend their appreciation especially to T. B. Lee and Don Crosby for their work in the design, construction, and testing of the Langmuir probe system; J. C. Pearl and Dr. E. G. Fontheim for valuable discussions on the theoretical aspects.

REFERENCES

1. Burt, D. A. "Rocket Instrumentation for Auroral Measurements—Black Brant AC 17.604," Scientific Report No. 7, Contract No. AF 19(628)-4995, AFCRL 67-0295, University of Utah, March 1967.

2. Pearl, J. C. "Studies Toward Development of a D-Region Probe," Final Report, ORA No. 05235-1-F, Space Physics Research Laboratory, University of Michigan, 1965.

3. Smith, L. G. "Ionization by Lyman-α in the E-Region at Sunrise," J. Atmos. Terr. Phys. 28, 119, 1966.

4. Balmain, K. G. "Plasma Probe Studies," Aeronomy Report No. 11, University of Illinois, May 1, 1966.

5. Su, C. H. and Ain A. Sonin. "Theory of Electrostatic Probe in a Moderately Ionized Gas," Phys. Fluids 8, 124, 1967.

6. Medicus, G. "Theory of Electron Collection of Spherical Probes," J. Appl. Phys. 32, 2512, 1961.

7. Kanal, M. "Theory of Current Collection of Moving Spherical Probes," Scientific Report No. JS-5, ORA No. 03484, 03599-9-S, Space Physics Research Laboratory, University of Michigan, 1962.

8. Sagalyn, R. C., M. Smiddy, and J. Wisnia. "Measurement and Interpretation of Ion Density Distribution in the Daytime F-Region," J. Geophys. Research 68, 199, 1963.

9. Nagy, A. F., L. H. Brace, G. R. Carignan, and M. Kanal. "Direct Measurements Bearing on the Extent of Thermal Non-Equilibrium in the Ionosphere," J. Geophys. Research 68, 6401, 1963.

10. Laframboise, J. G. "Theory of Spherical and Cylindrical Langmuir Probes in a Collisionless, Maxwellian Plasma at Rest," UTIAS Report No. 100, University of Toronto.

11. Mott-Smith and I. Langmuir. "The Theory of Collectors in Gaseous Discharges," Phys. Rev. 28, 727, 1926.

12. Bettinger, R. T. and E. H. Walker. "Relations for Plasma Sheaths about Langmuir Probes," Phys. Fluids 8, 748, 1965.

13. Hoegy, W. R. and L. H. Brace. "The Dumbell Electrostatic Ionosphere Probe: Theoretical Aspects," Scientific Report No. JS-1, ORA No. 03599-5-S, Space Physics Research Laboratory, University of Michigan, 1961.

14. Nagy, A. F. "Measurement of Charged Particle Parameters in the Lower Ionosphere," Status Report No. 3, ORA No. 07084-3-P, Space Physics Research Laboratory, University of Michigan, 1966.

15. Narcisi, R. S. and A. D. Bailey. "Mass Spectrometric Measurements of Positive Ions at Altitudes from 64 to 112 km," J. Geophys. Research 70, 3687, 1965.

16. Ulwick, J. C., W. Pfister, and K. Baker. "Results of Rocket Experiment in Auroral Absorption Events," Presented at the Eight COSPAR international Space Science Symposium. Also to be published in Space Research, Vol. 8.

17. Schulz, G. J. and S. C. Brown. "Microwave Study of Positive Ion collection by Probes," Phys. Rev. 98, 1642, 1965.

APPENDIX

ELECTRONIC SYSTEM TEST AND EVALUATION DATA

ELECTROSTATIC PROBE ELECTRONICS UNIT NO. 17.604

PURPOSE: Charge particle parameter measurement.

SENSITIVITIES (F.S.): .008 μA; 1.0 μA; 0.1 μA; 15 μA

NUMBER OF: DETECTORS 2, PROBES 1, OUTPUTS 2.

POWER REQUIREMENTS: 28 volts; 2.94 watts

HI ΔV: Mag. + 2.5 to -2.5 v, dV/dt 10 v/sec
Output Imp. 300 Ω

LO ΔV: Mag. + N/A to - N/A v, dV/dt N/A,
Output Imp. N/A Ω

Period: 495 sec.

Monitor Output Imp. 33 K Ω

ELECTRICAL CHARACTERISTICS OF DETECTORS

DETECTOR #1:

Range 1: .008 μA (F.S.), dE_o/dI_{in} 300 v/μA, Input Imp. 30 K Ω

Range 2: 1.0 A (F.S.), dE_o/dI_{in} 4.0 v/μA, Input Imp. 400 Ω

Voltage Ration of Range 1/Range 2 84.25

Output Imp. 2 K Ω, Limited at -.5 + 5.5 v.

Calibration Resistance 25 Meg, 2 Megr.

DETECTOR #2:

Range 1 .1 μA (F.A.), dE_o/dI_{in} 25 v/μA, Input Imp. 2.5 K Ω

Range 2 -15 μA (F.A.), dE_o/dI_{in} 33 v/μA, Input Imp. 33 Ω

Ratio of Range 1/Range 2 7.1

Output Imp. 2 K Ω, Limited at -.5 + 5.5 v.

Calibration Resistance 25 Megr. 2 Meg.

TIMERS:

MASTER: PERIOD 500 M and 25 M SEC IN SYNC. WITH N/A

RANGE: PERIOD 500 M and 50 M SEC TRIGGERED BY FF #2

DETECTOR: PERIOD 100 M and 1 SEC

CALIBRATION: ON: 100 M and 1 SEC INTERVALS: 100 M SEC

PROBE: PERIOD N/A SEC IN SYNC. WITH N/A

Unit No: 17.604 Date: 10/21/65

Sensitivity: .008, 1.0, .100, and 15 μ a Checked by D. F. CROSBY

Source Voltage and Current: 28 v and 105 MA

At Ambient:

Full Scale Output: 5.50 volts
$\Delta V_o/\Delta I_{in}$: Det #1 3.6 and, 303.5, Det #2 0.31 and, 2.2 volts/μA
Range Period: 50 Ms and 500 Ms
Calibration Period: 100 Ms and 1 sec
Ratio of Hi to Lo Current Ranges: Det #I 125, Det II 150

Temp. °C	Det #1						Det #2					
	Output Volts		$\Delta V_o/\Delta I_{in}$		Bias Level		Output Volts		$\Delta V_o/\Delta I_{in}$		Bias Level	
	I	II	I	II	I	II	I	II	I	II	I	II
25	5.50	5.50	303.5	3.6	2.68	0	5.50	5.50	22.75	.31	2.68	0

FLAGS: Range 1 (Hi.S) 2, Range 2 (Lo.S,0 Output Imp. 47 K
DET #1 2 DET #2 0 Output Imp. 47 K
HI ΔV N/A, LO ΔV N/A Output Imp. N/A

SIZE: 3" Dia 16-13/16" long

WEIGHT: 4767 GRAMS (10.5 lb incl. cable)

ΔV PERFORMANCE DATA

Unit No. 17.604 Date 10/21/65

Checked By D. F. Crosby

At Ambient:

Magnitude: + 2.5 v to -2.5 v
Period: 495 M/sec
Slope: HI 10 LO N/A slope, v/sec

Temp. °C	Period Milli Sec.	Magnitude +v	Magnitude -v	HI	LO
25	495	2.5	2.5	10.1 v/sec	
-15	476	2.3	2.5	10.25 v/sec	
50	489	2.42	2.4	9.5 v/sec	
25	25.5	2.5	2.5		
-15	24.5	2.5	2.45	square wave	
70	27	2.46	2.5		